

Original scientific paper

UDC 004.972:514(497.113)  
[https://doi.org/to\\_be\\_assigned](https://doi.org/to_be_assigned)

Received: October 23, 2025

Corrected: February 11, 2026

Accepted: March 02, 2026

**Ion Andronache**<sup>1\*</sup>

*\*Advanced Digital Archaeological-Historical Network, Alma Mater Europaea (AMEU) – ECM – Slovenska, Maribor, Slovenia; "Vasile Alecsandri" and "Alexandru Ioan Cuza" Secondary School, Braila, Romania; "Gheorghe Munteanu-Murgoci" National College, Braila, Romania*

## FRACTAL ANALYSIS FOR 2D AND 3D BINARY IMAGES

**Abstract:** We present a unified, letter-coded framework for interpreting 2D and 3D binary images that groups descriptors into a complementary triad: global complexity, fragmentation/disorder, and connectivity. Applied to the Banat Mountains, we analyze three layers: tree cover (2000–2021), cumulative forest loss (2001–2021), and annual forest loss (2001–2021), using a parsimonious portfolio of fractal and non-fractal indices (box-counting and related dimensions, the fragmentation family FFI/FFDI/FTI, lacunarity, and succolarity) and their 3D analogues. The fragmentation family complements class-level FRAGSTATS metrics (e.g., edge density, clumpiness) by isolating scaling-sensitive edge irregularity and tentacularity. Results converge across dimensions: tree cover behaves as a compact, nearly space-filling matrix with high, stable connectivity, low disorder, declining lacunarity, and modest, non-systemwide gains in succolarity; annual loss shows episodic spikes in disorder and transient connectivity with reduced anisotropy. In 3D, tree cover is nearly space-filling, cumulative loss is intermediate and filamentary, and annual loss is sparse, with succolarity meaningful only for the matrix. We conclude with a practical monitoring set that captures the triad while minimizing redundancy and outline sensitivity and transferability to other mountainous, heterogeneous regions in Southeastern Europe.

**Keywords:** fractal analysis, binary images, Banat Mountains, forest loss, tree cover, lacunarity, succolarity, fragmentation indices

## Introduction

Fractal analysis has emerged over the past decades as a cornerstone methodology in geographic and ecological sciences, offering robust tools for quantifying and interpreting the complexity of natural and anthropogenic landscapes. This mathematical framework is particularly effective in identifying self-similar structures and patterns across multiple scales, making it indispensable for uncovering spatial hierarchies, fragmentation, and other intricate features often overlooked by traditional methods (Milne, 1988; O'Neill et al., 1988; Halley et al., 2004; Gustafson, 2019).

---

1 andronacheion@email.su (corresponding author)  
Ion Andronache (<http://orcid.org/0000-0001-7693-9098>)

Its application becomes especially significant in heterogeneous regions like the Banat Mountains, located in southwestern Romania. Characterized by a dynamic interplay of natural processes and human activities, this area presents diverse land use, vegetation patterns, and geological formations. Understanding the spatial dynamics of such a multifaceted environment is critical for sustainable land management, biodiversity conservation, and environmental risk assessment. This is particularly relevant for the complex and often vulnerable mountainous landscapes of Southeastern Europe, such as the Banat Mountains, which form part of the Carpathian arch at the interface with the lower Danube corridor and the Dinaric ranges.

Fractal analysis bridges the gap between visual interpretation and quantitative precision, enabling researchers to extract meaningful insights from complex spatial datasets (Mandelbrot, 1982).

Despite its potential, fractal analysis remains underutilized in geographic research, particularly in the interpretation of binary images derived from geospatial data. Binary images - produced through remote sensing, digital elevation models (DEMs), and other tools - offer a simplified yet powerful representation of spatial features. When coupled with fractal methodologies, these images reveal nuanced patterns such as the distribution of forest patches, water bodies, or geomorphological structures (Milne, 1991; Turcotte, 1997). However, the integration of fractal indices into routine geospatial analyses is still in its early stages, underscoring the need for systematic approaches that combine theoretical innovation with practical applicability.

The primary objective of this study is to advance the application of fractal analysis in the interpretation of 2D and 3D binary images. The research focuses on both methodological advancements and practical insights. Specifically, it aims to refine existing fractal methodologies tailored to binary image analysis, apply these methods to case studies in the Banat Mountains, and demonstrate their broader implications for understanding landscape complexity and informing environmental decision-making.

Fractal analysis quantifies the delicate balance between order and chaos in natural systems, a dynamic reflected in the spatial arrangement of landscape features. By leveraging these insights, the study contributes to advancing cross-disciplinary research, spanning geography, ecology, and environmental management. Additionally, the findings offer a foundation for future studies to develop more sophisticated analytical tools, fostering a deeper appreciation of the inherent complexity of our natural world (Turcotte, 1997; Schertzer & Lovejoy, 2011; Newman et al., 2019).

By positioning fractal analysis as a pivotal approach to interpreting binary images, with the Banat Mountains as a testing ground, this research bridges theoretical innovation with practical implementation. It provides a methodological framework and actionable insights, enhancing our ability to analyze and manage complex landscapes effectively.

## **Materials and Methods**

The Banat Mountains present a dynamic and complex landscape where forested areas and patterns of forest loss interact intricately over time. To effectively capture and analyze these spatial dynamics, it is essential to employ robust geospatial and analytical methodologies. The framework outlined in this study integrates high-resolution satellite imagery

with advanced geospatial tools, enabling a detailed examination of tree cover and forest loss across the region. This section provides an overview of the data sources, preprocessing steps, and analytical methods employed to extract meaningful insights into forest dynamics, with a particular emphasis on reproducibility and applicability to similar landscapes.

### Study Area: Banat Mountains

The Banat Mountains, situated in southwestern Romania, are an integral part of the Western Carpathians and stand out as a region of ecological and environmental importance (Figure 1). Renowned for their heterogeneous topography, diverse vegetation, and intricate geological formations, these mountains span the counties of Caraș-Severin and Timiș. They encompass notable subranges such as the Semenic, Anina, and Almăj Mountains, each distinguished by its unique geomorphological characteristics and rich forest cover (Posea, 2005).

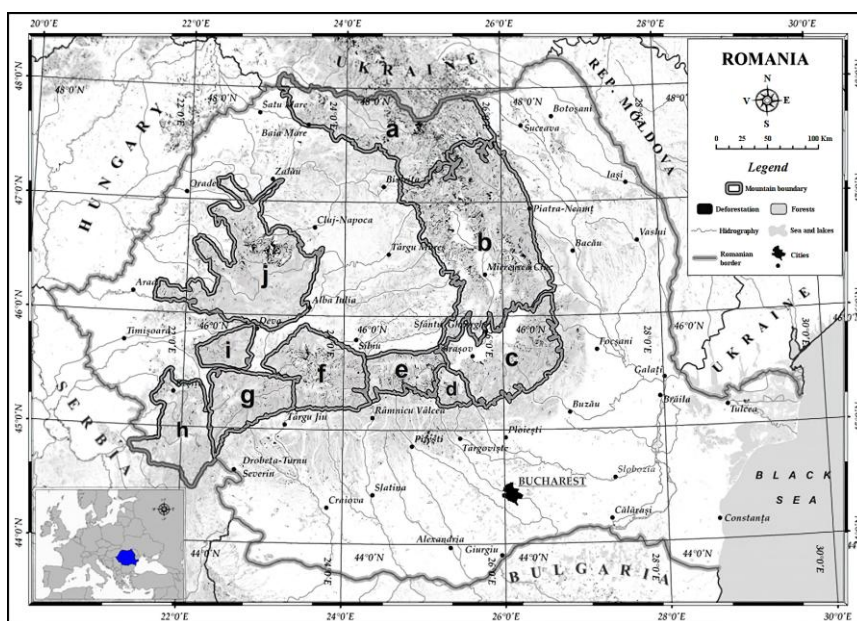


Fig. 1. Geographic location of the Romanian Carpathian groups, showing: (a) Northern Eastern Carpathians; (b) Central Eastern Carpathians; (c) Southern Eastern Carpathians; (d) Bucegi Mountains Group; (e) Făgăraș Mountains Group; (f) Parâng Mountains Group; (g) Retezat-Godeanu Mountains Group; (h) Banat Mountains; (i) Poiana Ruscă Mountains; (j) Apuseni Mountains.

Forests dominate the Banat Mountains, primarily consisting of extensive beech (*Fagus sylvatica*) stands and mixed deciduous forests. These forests cover roughly 37% of the Banat Mountains (Hansen et al., 2013) and serve as major carbon sinks supporting numerous plant and animal species. They also contribute to soil stabilization, water regulation, and climate moderation, underscoring their importance.

From a socio-economic perspective, the Banat Mountains have experienced a long history of human activities, including forestry, mining, and agriculture. While these industries have been central to the local economy, they have also triggered significant deforestation and land-use changes over the decades. Forest loss in this region arises from a combination of natural disturbances, such as wind throws and pest outbreaks, as well as anthropogenic

pressures, including logging, infrastructure development, and agricultural expansion (Knorn et al., 2013; Janda et al., 2017; Ianăș & Ivan, 2022; Cojocariu et al., 2024). Such pressures underscore the need for robust studies on forest dynamics and conservation strategies.

The Banat Mountains' forests have been the subject of numerous research efforts aimed at understanding biodiversity, conservation, and sustainable land use (Ianăș & Ivan, 2022; Petrișor et al., 2010; Ianăș, 2013; Artugyan, 2016). Given the region's complex forested landscape and its vulnerability to both natural and human-induced changes, it provides an ideal setting for applying advanced spatial analysis techniques. In particular, the use of fractal analysis offers a powerful approach to investigating forest loss and fragmentation patterns, facilitating a deeper understanding of the drivers and consequences of deforestation.

The Banat Mountains' ecological value and ongoing anthropogenic pressures make the region an ideal testbed for advanced spatial analysis. In this study, we quantify tree cover and forest loss using high-resolution satellite data and reproducible geospatial workflows, providing a framework applicable to Banat and transferable to similar mountainous landscapes. While biodiversity is acknowledged as an important ecological attribute of the Banat Mountains, the present study focuses strictly on structural forest properties (extent, fragmentation, and connectivity) derived from binary remote-sensing layers and does not directly quantify species diversity.

### ***Framework for Spatial Analysis of Tree Cover and Forest Loss***

We used the Global Forest Change (GFC) dataset (30 m spatial resolution) for 2000–2021 (Hansen et al., 2013). The 2000 layer provided baseline tree cover, while annual forest loss layers were available for 2001–2021.

Source rasters were distributed in WGS 84 (EPSG: 4326) and were reprojected to Dealul Piscului 1970 / Stereo 70 (EPSG: 31700) to match the study projection. We then clipped all layers to the study-area mask.

To enable stratified summaries, loss rasters were retained as categorical data with 22 classes (class 0 = no loss within the study area, classes 1–21 = annual loss from 2001 to 2021). The tree-cover raster was represented by 101 classes (0–100), each denoting percent tree cover at pixel level. All products preserve the native 30 m resolution.

Subsequent processing used ImageJ (Schneider et al., 2012) and standard GIS tools (QGIS Development Team, 2024). For binary classification, GeoTIFFs were converted to 8-bit images and thresholded in ImageJ (lower bound = 1, upper bound = 255), then converted to binary masks with 0 (background/non-forest) and 255 (foreground/forest) (Figure 2). This ensured compatibility with downstream fractal analyses.

Cumulative loss layers were generated by iterative summation of annual loss masks (e.g., cumulative 2002 = loss 2001 + loss 2002; ...; cumulative 2021 =  $\Sigma$  loss 2001–2021) using ImageJ's *Process* → *Image Calculator* (*Add*). Annual tree cover for 2001–2021 was obtained by differencing the 2000 baseline with cumulative loss up to each year (*Image Calculator* → *Difference*).

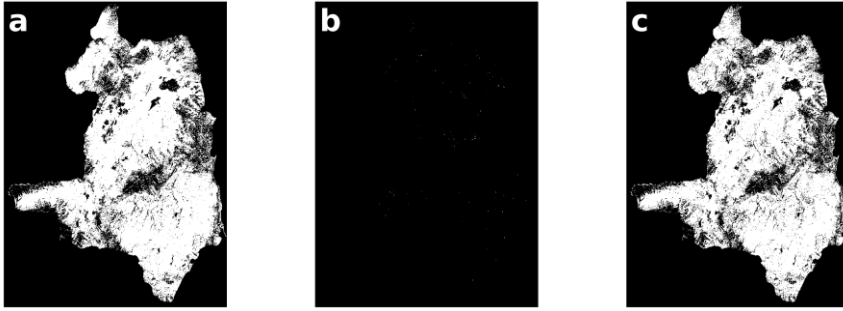


Fig. 2. Binary inputs used in the analyses.  
(a) Tree cover 2000; (b) Cumulative forest loss 2001-2021; (c) Tree cover 2021.

The resulting binary ensembles (tree cover, cumulative loss) constitute a reproducible and transferable workflow: given equivalent inputs, the same steps yield comparable products for other regions.

### **Fractal Methods for Binary Image Analysis**

To analyze the complexity of spatial structures in binary images, robust mathematical methods are required to capture geometric characteristics and spatial distributions across multiple scales. Fractal methods provide a comprehensive set of tools that enable the quantification of variability and fine structural details, contributing to a deeper understanding of both natural and anthropogenic systems.

One of the most widely used techniques for estimating the fractal dimension of binary structures is the *box-counting method* (Sasaki et al., 1994; TruSoft International, 1997; Zmeškal et al., 2011; Karperien, 2015; Vuidel et al., 2022; Ahammer et al., 2023). This technique involves covering the image with square boxes of varying sizes (powers of 2) and counting the number of boxes needed to cover the objects. The relationship between the box count and box size is plotted on a log-log graph, where the slope determines the fractal dimension (Sarkar & Chaudhuri, 1992; Jin et al., 1995). Raster box scanning ensures systematic image coverage, enabling assessments of structural complexity and fragmentation.

The *pyramid dimension* extends the box-counting method by iteratively reducing image size, making it particularly suitable for non-uniform image dimensions. At each step, the pixel count of the objects is recorded, and the log-log relationship between pixel count and reduced image size estimates the fractal dimension (Ahammer & Mayrhofer-Reinhartshuber, 2012; Mayrhofer-Reinhartshuber et al., 2013). This method eliminates truncation errors associated with non-square images, providing precise evaluations of structural fragmentation.

The *correlation dimension* evaluates the complexity of pixel distributions by analyzing pairwise relationships at varying distances. The function calculates correlations at multiple scales, and the log-log relationship between correlated pairs and their distances provides the fractal dimension (Grassberger & Procaccia, 1983). Methods such as raster and sliding box scanning facilitate both global and local distribution analyses. *Radial analysis* examines the spatial distribution of pixels relative to a central point, typically the object's center of mass. Concentric circles with increasing radii are drawn, and the pixel count within each circle is measured. The log-log relationship between pixel count and radius determines the fractal dimension (Vuidel et al., 2022), making it ideal for analyzing radial behaviors and

concentric distributions. The *sandbox analysis method* analyzes pixel distributions within incrementally larger boxes centered on individual reference points. The log-log relationship between box size and pixel count determines the fractal dimension (Vuidel et al., 2022), offering valuable insights into spatial clusters and complex distributions.

To quantify irregularity and fragmentation, the *Fractal Fragmentation Index* (FFI) plays a critical role. It is calculated as the difference between the fractal dimension of the mass (spatial occupancy) and the fractal dimension of the perimeter (contour complexity) (Andronache et al., 2016). Lower FFI values indicate highly fragmented structures, while higher values suggest compact objects. The *Fractal Fragmentation and Disorder Index* (FFDI) extends this concept by incorporating the informational dimension ( $D_i$ ), offering a broader perspective on heterogeneity and fragmentation (Peptenatu et al., 2023). The *Fractal Tentacularity Index* (FTI) quantifies the branching and tentacular extensions of binary objects. Calculated as the difference between the convex hull FFI and FFI, it provides insights into the structural complexity of geometric forms (I. Andronache et al., 2024). Our fragmentation family (FFI/FFDI/FTI) complements class-level FRAGSTATS metrics (e.g., edge density, clumpiness) by explicitly isolating scaling-sensitive edge irregularity (via FFDI) and tentacularity (via FTI) (McGarigal et al., 2012a).

The *perimeter-area dimension* complements these analyses by evaluating contour complexity and determining the degree of fragmentation through the relationship between an object's perimeter and area (Mandelbrot, 1982). Similarly, the mass-radius dimension analyzes pixel mass variation as a function of radial distance, employing concentric circles to measure cumulative pixel mass (Landini & Rippin, 1993). The *Minkowski dimension* uses morphological dilation, where objects expand iteratively by adding pixels at the edges, and the total occupied area is measured. The log-log relationship between dilation size and occupied area determines the fractal dimension (Dubuc et al., 1989).

The *Tug of War dimension* introduces a statistical perspective by analyzing surface variations across scales. It is employed to identify fine details and assess spatial irregularities (Reiss et al., 2016).

*Succolarity* ( $\sigma$ ) estimates directional "permeability" of a binary image (black = traversable, white = barrier) by scanning the grid along a chosen direction under a virtual pressure from the source edge;  $\sigma \in [0,1]$ , higher means easier percolation. We report  $\sigma$  for top→down, bottom→top, left→right, right→left, plus their mean. Raster box scanning ensures systematic coverage and comparability across images (de Melo & Conci, 2013). *Potential (reservoir) succolarity* ( $\sigma_p$ ) is the theoretical upper bound of percolation given by the global share of traversable pixels, independent of direction, and serves as the reference ceiling against which realized  $\sigma$  is evaluated. *Delta succolarity* ( $\Delta\sigma$ ) is the unrealized connectivity margin defined as  $\Delta\sigma = \sigma_p - \sigma$  (per direction or mean); larger values indicate occluded mass, bottlenecks, or disconnected lobes that would become active if barriers were removed or corridors added (Andronache, 2024).

For succolarity runs targeting patch-to-patch forest connectivity, binary masks were inverted so that forest = black (traversable) and non-forest = white (barrier), ensuring that  $\sigma$  reflects connectivity among forest patches rather than void permeability. Reservoir and  $\Delta$ -succolarity were computed consistently with this convention.

These methodologies used for analyzing 2D binary images have been directly extended to 3D contexts, enabling researchers to explore volumetric structures with the same precision. The 3D fractal analysis methods (Andronache et al., 2024) include the 3D Box Counting Dimension, 3D Correlation Dimension, 3D Fractal Fragmentation Indices, 3D Generalised Fractal Dimensions, 3D Lacunarity, 3D Minkowski Dimension, 3D Succolarity, and 3D Tug of War Dimension. These approaches enable the quantification of volumetric complexity, connectivity, and spatial variability in 3D binary datasets, making them indispensable for analyzing geological formations, biological tissues, and spatial networks.

### *The Relevance of Fractal Indices in Spatial Analysis*

Fractal analysis, with its diverse methodologies, offers profound insights into structural and spatial characteristics in binary images. The relevance of these methods spans several primary directions, each addressing specific analytical needs.

For global image analysis, techniques like box-counting, Minkowski dimension, and fragmentation indices (FFI and FFDI) are invaluable. They assess overall structural features such as fragmentation and contour complexity, providing key indices of global spatial organization.

For detailed analysis of textures and fragmentation, methods such as lacunarity, succolarity, and the Fractal Tentacularity Index (FTI) excel. These indices capture distribution heterogeneity and structural connectivity, especially in analyzing natural surface morphologies.

Contour characterization is another critical focus. Methods such as perimeter-area dimension, radial analysis, and Walking Divider quantify contour complexity and geometric behaviors, highlighting structural irregularities.

Beyond 2D applications, the adaptation of fractal indices to 3D enhances their relevance in volumetric analyses. 3D methods, including 3D Box Counting and 3D Generalised Dimensions, are crucial for studying geological formations, 3D forest structures, and biological tissues. These tools bridge the gap between planar and volumetric datasets, providing continuity across dimensions.

Finally, multifractal analysis through generalized dimensions captures the variability of complex distributions, making it particularly suitable for diverse systems like natural landscapes and spatial networks.

By integrating these techniques, fractal analysis serves not only as a descriptive tool but also as a powerful analytical framework. Its applications span environmental science, ecology, and resource management, offering actionable insights and fostering data-driven decision-making.

### ***Reproducibility***

All data, scripts, and parameter files (thresholds, structuring elements, box ladders, fitting ranges) are provided in the supplementary material, together with a letter legend (a–af) (Table 1). Given identical inputs, the workflow reproduces the reported figures and tables; progress logging, timing, and verbose reporting are enabled for auditability. Figures 3–5 that reference letters (a–f) use the common legend in Table 1.

Table 1. Letter–metric legend used throughout the figures 3–5 (a–af).

Family	Code	Metric (software)	Family	Code	Metric (software)
Global complexity	a	Box-counting dimension (ComsystanJ 1.2.0)	Global complexity	r	Mass radius dimension (ComsystanJ 1.2.0)
	b	Box-counting dimension (Harmonic and Fractal Image Analyzer 5.5.28 - White+BlackWhite)		s	Mass dimension (Benoit 1.31)
	c	Box-counting dimension (Fractal Analysis System 3.4.7)		t	Perimeter-area dimension (ComsystanJ 1.2.0)
	d	Box-counting dimension (Benoit 1.31)		u	Tug-of-war dimension (ComsystanJ 1.2.0)
	e	Box-counting dimension (Fractalyse 3.0)		v	Fractal anisotropy index (horizontal and vertical direction) (ComsystanJ 1.2.0)
	f	Box-counting dimension (Harmonic and Fractal Image Analyzer 5.5.28 - BlackWhite)		x	Fractal anisotropy index (Mean of 4 radial directions [0-180°]) (ComsystanJ 1.2.0)
	g	Box-counting dimension (Harmonic and Fractal Image Analyzer 5.5.28 - Black+BlackWhite)			
	h	Pyramid dimension (ComsystanJ 1.2.0)		Fragmentation/disorder	y
	i	Dilation dimension (Fractalyse 3.0)	z		Fractal Fragmentation and Disorder Index (FFDI) (ComsystanJ 1.2.0)
	j	Minkowski dimension (ComsystanJ 1.2.0)	aa		Fractal Tentacularity Index (FTI) (ComsystanJ 1.2.0)
	k	Radial dimension (Fractalyse 3.0)	Lacunarity/Succolarity	ab	Lacunarity (Roy & Perfect) (ComsystanJ 1.2.0)
	l	Information dimension (ComsystanJ 1.2.0)		ac	Lacunarity (Sengupta & Vinoy) (ComsystanJ 1.2.0)
	m	Information dimension (Benoit 1.31)		ad	Succolarity (ComsystanJ 1.2.0)
	n	Correlation dimension (Fractalyse 3.0)		ae	Succolarity (reservoir) (ComsystanJ 1.2.0)
	o	Correlation dimension (ComsystanJ 1.2.0)		af	Delta succolarity ( $\Delta$ -succolarity) (ComsystanJ 1.2.0)
p	Directional correlation dimension (horizontal and vertical direction) (ComsystanJ 1.2.0)				
q	Directional correlation dimension (Mean of 4 radial directions [0-180°]) (ComsystanJ 1.2.0)				

Note. Families and code ranges used across figures 3–5: Global complexity (a–x), Fragmentation/disorder (y–aa: FFI, FFDI, FTI), Heterogeneity–connectivity (ab–af: lacunarity ab–ac; succolarity ad–ae;  $\Delta$ -succolarity af).

## Results

We analysed forest-cover dynamics in the Banat Mountains using three datasets: tree cover (2000–2021), cumulative loss (2001–2021), and annual loss (2001–2021). We computed a broad, but structured, set of indicators grouped into four families that capture the complexity-fragmentation-connectivity triad.

- Global structural complexity (fractal dimensions). Box-counting (using ComsystanJ, HarFA W+BW, HarFA BW, HarFA B+BW, Benoit, Fractalyse, Fractal Analysis System for Windows), Pyramid dimension, Dilation dimension, Minkowski dimension, Radial dimension, Informational dimension (using ComsystanJ and Benoit), Correlation dimension (ComsystanJ and Fractalyse variants), Directional correlation dimensions (horizontal/vertical and the mean of four radial directions), Mass radius, Mass, Perimeter–area, Tug-of-war, and the Fractal anisotropy indices.

- Fragmentation and disorder. Fractal Fragmentation Index (FFI), Fractal Fragmentation and Disorder Index (FFDI), Fractal Tentacularity Index (FTI).
- Lacunarity (Roy & Perfect; Sengupta & Vinoy) and Succolarity (reservoir variants and Delta succolarity).

These indicators resolve complementary temporal behaviours: annual loss emphasises event-like shocks, cumulative loss expresses long-term reorganisation, and tree cover provides the stable background against which both processes unfold.

### ***General overview across datasets***

Across datasets, the core 2D dimensions in tree cover (box-counting, pyramid, Minkowski) remain very high and nearly constant at  $\approx 1.95$ , confirming a compact, continuous matrix; in cumulative loss they increase steadily from  $\approx 0.94$  (2001) to  $\approx 1.30$  (2021), indicating progressive complexification as yearly losses accumulate; in annual loss they fluctuate strongly, consistent with episodic disturbance. Fragmentation indices (FFI, FFDI, FTI) rise monotonically for cumulative loss, showing that accumulation is not only quantitative but also qualitative as edges become more irregular and more tentacular; in annual loss they show pronounced peaks in 2004, 2008, 2012, 2016, and 2020, captured more sharply by FFDI/FTI than by global dimensions; in tree cover, fragmentation remains low and stable with a subtle divergence - FFI decreases slightly while FFDI/FTI increase slightly - revealing method-dependent sensitivities under near-constancy. In practice, FFI/FFDI/FTI complement class-level summaries (edge density, clumpiness) by targeting scaling-sensitive edge irregularity and tentacular extension.

Regarding heterogeneity and connectivity, lacunarity declines in cumulative loss (forest gaps become fewer/smaller and less heterogeneous overall), while succolarity - interpreted as connectivity among forest patches - increases modestly and remains below connectivity at the landscape scale; in annual loss, lacunarity varies and succolarity shows transient increases in peak years (2004, 2008, 2012, 2016, 2020); in tree cover, lacunarity remains low (low heterogeneity of gaps) and succolarity remains high and stable (strong and sustained patch connectivity), consistent with a largely continuous forest matrix.

### ***Annual forest loss (2001–2021)***

Fractal dimensions exhibit pronounced interannual oscillations, and direction-sensitive metrics - Directional correlation (H/V) and fractal anisotropy indices (H/V; four-direction mean) - decline in peak-loss years, indicating erosion of directional coherence as loss geometries become less elongated or aligned; aggregated across the family, the overall linear trend is mildly negative, punctuated by large deviations in shock years (2004, 2008, 2012, 2016, 2020). Fragmentation indices (FFI, FFDI, FTI) peak in those same years, capturing episodic disorder and tentacular outlines that global dimensions only partly reflect, underscoring their complementarity.

Lacunarity is variable with a modest downward tendency - implying a slight overall decrease in the heterogeneity of forest-gap distribution - while succolarity shows transient increases in the peak years, pointing to short-lived connectivity channels that momentarily traverse the background matrix without consolidating into persistent networks. The correlation architecture partitions into three loosely linked clusters - global complexity, fragmentation/disorder, and a third combining heterogeneity and connectivity (lacunarity/succolarity) - with cross-family correlations that are heterogeneous and generally weaker than in the cumulative regime, consistent with event-driven dynamics; positive associations frequently pair Minkowski, Radial,

or Informational (Benoit) dimensions with FFDI/FTI, whereas negative associations often link lacunarity (Roy & Perfect or Sengupta & Vinoy) with box-counting (Benoit/Fractalyse) or Minkowski dimensions. Decoupling is most evident in shock years, when Directional correlation and anisotropy indices diverge from the box-counting core, evidencing loss of anisotropy even as global complexity remains elevated.

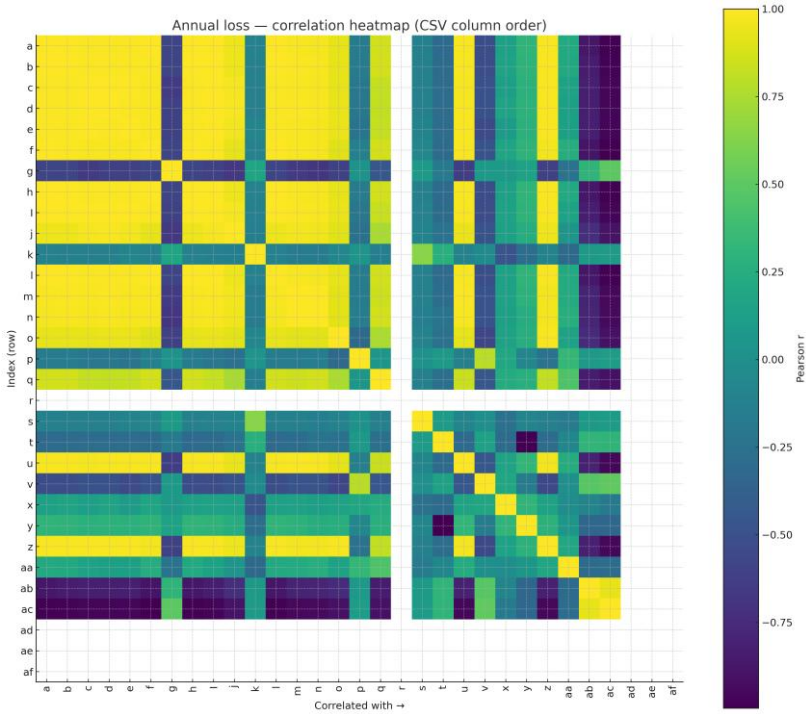


*Fig. 3. Annual forest loss (2001-2021): correlation heatmap. Pairwise Pearson correlations among the letter-coded indices (Table 1). Three loose clusters emerge, global complexity, fragmentation/disorder, and heterogeneity-connectivity (lacunarity-succolarity), with cross-family links that strengthen episodically in disturbance years.*

Figure 3 presents the annual forest-loss correlation heatmap, revealing a three-cluster structure - global complexity, fragmentation/disorder, and heterogeneity-connectivity (lacunarity-succolarity) - with cross-family links that strengthen episodically in disturbance years.

**Cumulative forest loss (2001–2021): progressive complexification and tightening relations**

Fractal dimensions rise steadily from  $\approx 0.94$  in 2001 to  $\approx 1.30$  in 2021, with the strongest positive trends for Radial, Informational (Benoit), Box-counting variants (Benoit, Fractalyse, HarFA BW, HarFA W+BW), Dilation, and Minkowski, documenting sustained complexification of the cumulative mosaic. Fragmentation metrics FFI, FFDI, and FTI also increase, indicating progressively more irregular and tentacular edges in step with the rising global complexity. Lacunarity declines clearly, meaning forest gaps become fewer or smaller and less heterogeneous overall, while succolarity increases slightly and systematically, suggesting a modest rise in patch-to-patch connectivity that remains below connectivity at the landscape scale.

Relations tighten in this long-term regime, with within-family coherence near unity for lacunarity ( $\approx 0.997$  agreement between Roy and Perfect and Sengupta and Vinoy), moderate for fragmentation and disorder ( $\approx 0.58$ ) and for fractal dimensions ( $\approx 0.42$ ), while across families global complexity correlates strongly and positively with fragmentation and strongly and negatively with lacunarity with mean  $r \approx -0.87$ . Representative positive pairs link Radial, Informational (Benoit), Box-counting (Benoit and Fractalyse), and Dilation with FFDI and FTI, whereas the strongest negative pairs link lacunarity from both estimators with Minkowski, Box-counting, and Informational or Correlation dimensions and also with FFDI and FTI.

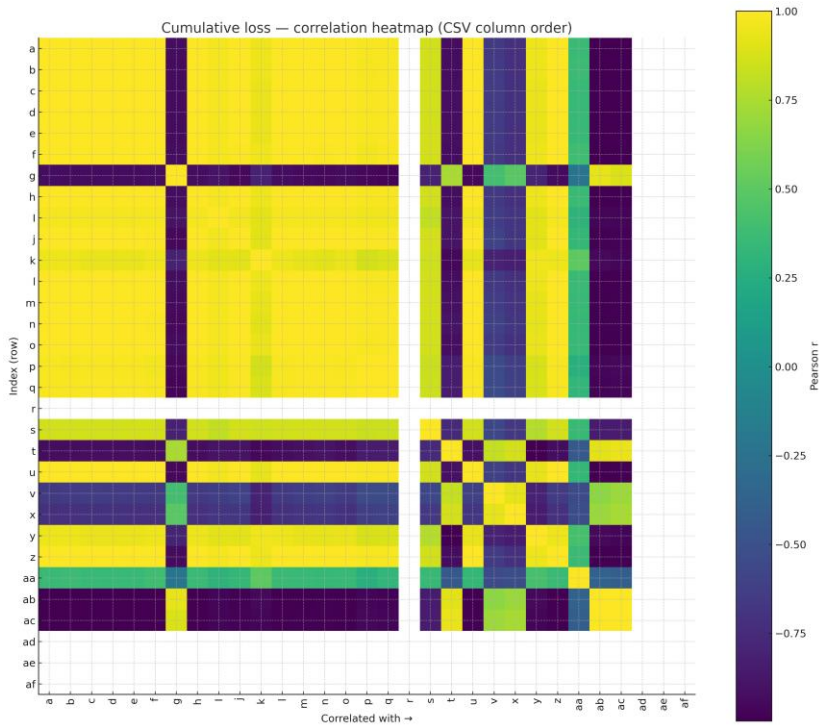


Fig. 4. Cumulative forest loss (2001-2021): correlation heatmap.

Pairwise Pearson correlations among the letter-coded indices (Table 1). Relations tighten: global complexity positively couples with fragmentation/disorder, while both strongly oppose lacunarity; internal agreement within lacunarity approaches unity.

Figure 4 presents the cumulative forest-loss correlation heatmap, highlighting near-unity coherence within lacunarity, a strong positive coupling between global complexity and fragmentation/disorder, and a strong negative coupling between global complexity and lacunarity.

**Tree cover (2000/2001–2021): stable background and method-specific nuances**

Box-counting, Pyramid, and Minkowski remain very high and nearly constant ( $\approx 1.95$ ), consistent with a continuous forest matrix; fragmentation levels are low and stable, with a subtle split in which FFI decreases slightly while FFDI and FTI increase slightly - reflecting distinct fragmentation definitions in a low-variance background (FFI is more sensitive to the disappearance/consolidation of larger patches, whereas FFDI/FTI emphasize fine-scale branching/irreg-

ularity). Regarding heterogeneity and connectivity, lacunarity remains low and stable - indicating low and steady heterogeneity in the spatial distribution of forest gaps - while succolarity remains high and largely stable, with a slight downward drift, consistent with strong patch-to-patch connectivity in a mostly continuous forest matrix.

Low variance dampens coherence compared with cumulative loss: mean within-family  $r$  is  $\approx 0.20-0.30$  for fractal dimensions and  $\approx 0.33$  for lacunarity; between families, lacunarity versus global complexity is generally negative, and global complexity versus fragmentation is weakly positive on family means but splits at the pair level because FFI often moves differently from FFDDI/FTI; under near-constancy, pairwise correlations can span a broad range ( $\approx -0.99...1.00$ ) due to method-specific sensitivities.

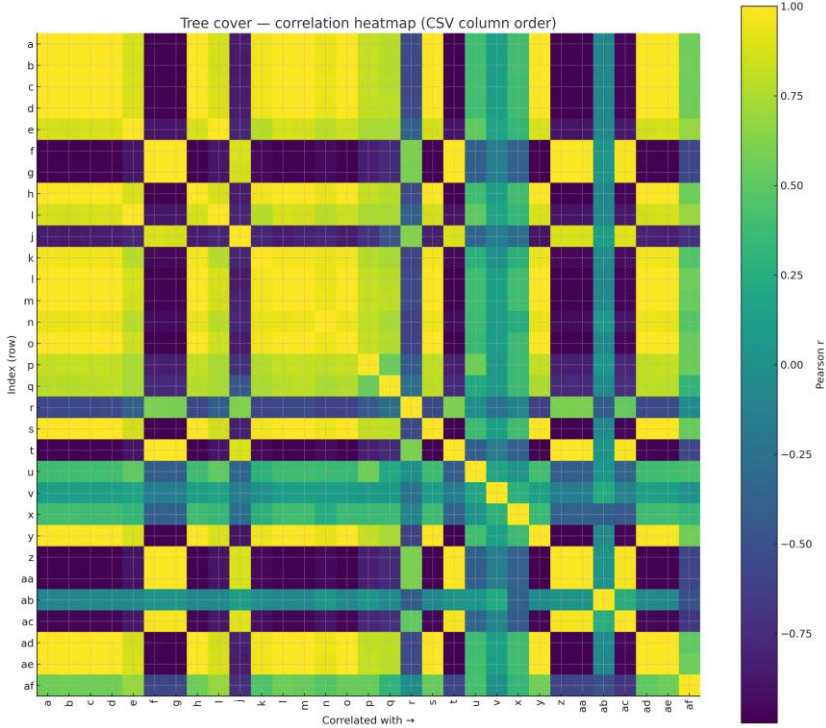


*Fig. 5. Tree cover (2000-2021): correlation heatmap. Pairwise Pearson correlations among the letter-coded indices (Table 1). Under low variance, correlations are damped; global complexity remains negatively associated with lacunarity, and fragmentation metrics show method-dependent nuances (FFI vs. FFDDI/FTI).*

Figure 5 presents the tree-cover correlation heatmap, illustrating dampened correlations under low variance, a persistent negative association between global complexity and lacunarity, and method-dependent nuances among fragmentation metrics (FFI vs. FFDDI/FTI).

***Integrated perspective and implications***

The time-series interpretation and the correlation architecture converge on a single process narrative in which, in the annual regime driven by events, disturbance shocks tran-

siently increase disorder and connectivity (succolarity) while eroding anisotropy, with clusters remaining loose and cross-family links episodic; in the cumulative regime, relations tighten and global complexity rises alongside fragmentation and disorder, while heterogeneity (lacunarity) declines and connectivity (succolarity) increases modestly without reaching landscape-scale connectivity; in the tree-cover background, stability suppresses correlations and makes method-specific differences among fragmentation indices most visible, with FFI diverging subtly from FFDI and FTI.

For parsimonious monitoring, a representative box-counting implementation such as Fractalyse or Benoit together with an informational or correlation dimension captures global complexity robustly; FFDI serves as a reliable proxy for branching irregularity, FTI emphasizes tentacular extension, lacunarity in the Roy and Perfect formulation compactly summarizes heterogeneity in the spatial distribution of forest gaps, and a succolarity variant is valuable whenever patch-to-patch connectivity is of particular interest.

### ***3D analysis of binary layers (Banat Mountains): tree cover, cumulative loss, and annual loss***

We quantified 3D structure on the three binary layers - tree cover, cumulative loss, and annual loss - using a mixed set of volumetric complexity, fragmentation/disorder, tentacularity, heterogeneity (lacunarity), morphology-derived, and connectivity (succolarity) descriptors, and both the 3D box-counting dimension (ComsysstanJ) and the 3D correlation dimension yield the same ordering, tree cover >> cumulative loss > annual loss, with tree cover nearly space-filling (Box-counting 3.02629, Correlation 2.80701), cumulative loss moderately complex (1.68721; 1.73301), and annual loss sparse (0.80838; 0.98797), confirming the dominance of the forest matrix in 3D while loss features remain comparatively thin or discrete; fragmentation and disorder align with this picture, as 3D FFDI separates cumulative loss (1.75119) and tree cover (1.71958) from annual loss (0.92367), whereas 3D FTI peaks for cumulative loss (1.03279) and is lower for annual loss (0.80541) and tree cover (0.56346), indicating that multi-year loss structures develop more elongated and branching filaments than within-year loss or the compact matrix, and 3D FFI is near-zero for cumulative (0.00313) and annual loss (0.00000) but clearly non-zero for tree cover (0.41288), consistent with fragmentation expressed primarily in voids within the dominant phase; heterogeneity assessed via 3D Roy & Perfect lacunarity is high for annual loss (1.67938) and cumulative loss (1.58841) and low for tree cover (0.37186), so loss layers exhibit patchy, clustered gap distributions whereas the forest matrix is comparatively homogeneous; a morphology-derived complexity score reported by the software as “3D Minkowski dimension” is largest for annual loss (5.90569), followed by cumulative loss (4.60127), and smallest for tree cover (1.57890), which we interpret as morphology-based complexity rather than a classical fractal dimension since values exceed the embedding bound and we document the computation in Methods; connectivity metrics based on succolarity are meaningful for tree cover only and indicate robust, near-isotropic connectivity with Succolarity 0.63131, Reservoir 0.59748,  $\Delta$ Succolarity 0.03383, and Anisotropy of succolarity 0.04723, while for loss layers the values are NaN, consistent with non-connectivity, sub-critical structures at the analyzed resolution; taken together, the Banat Mountains’ forest behaves in 3D as a dense, nearly Euclidean matrix with high space-filling dimensions, strong connectivity, low lacunarity, and low tentacularity, whereas loss layers are sparse and heterogeneous - annual loss is the most lacunar and, under the tool’s Minkowski score, the most morphologically intricate, cumulative loss shows the most filamentary organization (highest FTI) and intermediate complexity, yet neither achieves bulk connectivity - and

these outcomes mirror the 2D picture of a stable, connected forest background punctuated by localized openings that, when aggregated across years, form more elongated conduits without reaching system-spanning connectivity; we report NaN wherever succolarity descriptors are undefined due to the absence of a spanning phase.

The organisation of the forest mosaic has changed more than the total amount of cover. Loss patterns became more intricate and more irregular, gaps are on average less lacunar, and void connectivity rises episodically without becoming pervasive at landscape scale. This consolidated evidence strengthens the complexity-fragmentation-connectivity triad as a unified framework for interpreting forest dynamics in the Banat Mountains.

## **Discussion**

This study set out to understand how structural complexity, fragmentation/disorder, and connectivity co-evolve in the Banat Mountains by analysing three complementary layers: tree cover (2000–2021), cumulative forest loss (2001–2021), and annual forest loss (2001–2021). The results demonstrate that the three layers illuminate distinct but interlocking aspects of landscape dynamics, and that no single family of indices suffices to capture the full signal of change.

### ***Complementarity of 2D index families across temporal regimes***

The three temporal regimes express different processes and therefore privilege different indicators. In the continuous tree-cover matrix, global fractal dimensions remain very high and nearly constant ( $\approx 1.95$ ), characteristic of a compact, near space-filling pattern. Fragmentation/disorder metrics (FFI, FFDI, FTI) stay low but show small method-dependent drifts: a slight decrease in FFI alongside slight increases in FFDI/FTI, consistent with their different sensitivities under low variance (FFI tracking attrition of larger aggregates; FFDI/FTI emphasizing fine-scale branching/irregularity).

In cumulative loss, the long-term signal is clear and coherent: global dimensions increase steadily ( $\sim 0.94 \rightarrow \sim 1.30$ ), FFI/FFDI/FTI rise in tandem, lacunarity (heterogeneity of gaps) declines, and succolarity (connectivity among forest patches) increases modestly without approaching a connecting network at landscape scale. These patterns indicate qualitative reorganisation, not only quantitative loss: edges become more intricate and tentacular, while the traversable phase becomes slightly more connected.

In annual loss, event-driven variability dominates. Fragmentation/disorder metrics spike in the disturbance years 2004, 2008, 2012, 2016, 2020, while directional metrics (Directional correlation, fractal anisotropy indices) drop, signalling erosion of anisotropy during shocks. Lacunarity shows transient spikes in these years (on top of a slight overall downward tendency), and succolarity increases transiently, pointing to short-lived connectivity channels that puncture the matrix but do not persist. This asymmetry confirms that short-term diagnostics must include connectivity-focused indices, not only global complexity (Andronache et al., 2019).

Taken together, the indices form a complementary triad: global complexity summarizes the backbone of spatial organisation; fragmentation/disorder isolates the geometry of rupture; lacunarity quantifies the heterogeneity of forest gaps, while succolarity quantifies connectivity among forest patches. This division of labour is visible in Figures 3-5 and

matches prior reports on directional succolarity and  $\Delta$ -succolarity as proxies for intermittency of passage channels in fragmented matrices (Andronache, 2024; Diaconu et al., 2024).

### ***Correlation architecture***

In the cumulative-loss layer, heterogeneity (lacunarity; Roy & Perfect, Sengupta & Vinoy) shows near-unity internal agreement (mean within-family  $r \approx 0.997$ ), fragmentation/disorder exhibits moderate cohesion ( $\approx 0.58$ ), and fractal dimensions cohere at a comparable, moderate level ( $\approx 0.42$ ). Between families, global complexity is strongly and positively coupled with fragmentation/disorder, while its coupling with heterogeneity (lacunarity) is strongly negative (mean  $r \approx -0.87$ ). Together these relations crystallise a structural trade-off: as accumulated loss becomes more space-filling and edge-rich, relative gap size/variance declines, and connectivity (succolarity) increases only modestly - remaining below connectivity at landscape scale.

In the annual-loss layer, three clusters recur - global complexity, fragmentation/disorder, and a heterogeneity-connectivity cluster - yet cross-family links are episodic. The strongest positive pairs often link Minkowski, Radial, or Informational (Benoit) to FFDI/FTI, whereas the strongest negatives typically pit lacunarity (either estimator) against Box-counting (Benoit/Fractalysse) or Minkowski. Crucially, Directional correlation and anisotropy indices decouple from the Box-counting core in shock years, quantifying directional breakdown that global dimensions do not fully resolve; this echoes prior reports on the event sensitivity of combined fractal–GLCM descriptors (Andronache et al., 2019).

In the tree-cover layer, near-constancy of the matrix damps correlations across the board (e.g., mean  $r \approx 0.20$ – $0.33$  within families), making methodological contrasts more visible than in dynamic regimes. Negative associations between heterogeneity (lacunarity) and global complexity persist, as expected for compact patterns.

Overall, the correlation structure across layers reinforces the process interpretation: annual shocks yield transient disorder and connectivity gains with loss of anisotropy; cumulative reorganisation tightens the positive coupling of complexity with disorder and the negative coupling with heterogeneity; the stable background exposes definition-level differences among fragmentation metrics.

### ***Added value and caveats of the 3D extension***

Tree cover reaches very high 3D Box-counting (3.02629) and Correlation (2.80701) values, confirming a dense, coherent volumetric structure. Cumulative loss sits at intermediate complexity (3D Box-counting = 1.68721; 3D Correlation = 1.73301) but with elevated disorder (FFDI = 1.75119; FTI = 1.03279), suggesting irregular volumetric fragmentation. Annual loss shows very low volumetric complexity (3D Box-counting = 0.80838; 3D Correlation = 0.98797), consistent with episodic, structurally weak volumes. Notably, succolarity was undefined for loss volumes because no spanning phase was present at the analyzed resolution, reinforcing that surface-visible gaps often lack volumetric robustness to support connectivity (Diaconu et al., 2024). The 3D extension therefore corroborates the triad - complexity, fragmentation/disorder, lacunarity/succolarity - as a jointly necessary lens on structural change (Andronache, 2024).

### ***Fragmentation–connectivity interplay***

The joint evolution of indices points to a dual process. In cumulative loss, edge proliferation and tentacular outlines (rising FFDI/FTI) co-occur with declining lacunarity (lower

heterogeneity of forest gaps) and modest increases in succolarity (patch-to-patch connectivity), yielding a denser, more edge-rich loss mosaic that is only slightly more connected and remains sub-connecting at landscape scale. At yearly scales, disturbance shocks generate temporary connectivity channels and reduce anisotropy; these effects dissipate as the system relaxes toward background conditions. In 3D, both annual and cumulative losses are sparse, which helps explain why 2D succolarity gains remain modest and non-connected. This interpretation aligns with the use of directional succolarity and  $\Delta$ -succolarity to approximate connectivity and the intermittency of passage channels in fragmented forest matrices (Andronache, 2024; Diaconu et al., 2024).

### ***Relation to previous work***

Regional studies have largely relied on 2D metrics - box-counting, lacunarity, and perimeter–area scaling - together with landscape-metric toolkits such as FRAGSTATS (McGarigal et al., 2012a). Within this context, our fragmentation family (FFI/FFDI/FTI) is designed to complement class-level FRAGSTATS metrics by explicitly isolating scaling-sensitive edge irregularity (via FFDI) and tentacularity (via FTI). Our tree-cover results reproduce the expected stability of global fractal dimensions and the mixed inter-metric correlations under low variance (mean  $r \approx 0.27$ ; range  $-0.99 \dots 1.00$ ), consistent with prior lacunarity work showing that heterogeneity can vary independently of fractal dimension and is best assessed multi-scalar (Plotnick et al., 1993). For cumulative loss, we likewise observe near-unity internal cohesion for lacunarity ( $\approx 0.997$ ) and a strong negative coupling with global complexity ( $\approx -0.87$ ), alongside moderate cohesion among fragmentation/disorder ( $\approx 0.58$ ), in line with landscape-pattern theory and reviews warning about method choice and interpretation in ecological fractal analysis (McGarigal et al., 2012b). At annual scales, spikes in fragmentation and succolarity-based connectivity mirror the event sensitivity documented when combining fractal and texture descriptors (e.g., GLCM features) (Haralick et al., 1973). Beyond replication, this study extends the literature by integrating newer indicators (like FTI) and adding a 3D volumetric perspective that can be framed with integral-geometry morphology (Minkowski dimension) alongside correlation-dimension analyses (Michielsen & De Raedt, 2001). Finally, the connectivity interpretation resonates with connection-based views of critical scales and network formation in fragmented landscapes (Keitt et al., 1997). Our results align well with the cited literature. Turner (2010) emphasized that disturbance pulses can produce transient increases in landscape heterogeneity and structural complexity, consistent with the fragmentation/disorder spikes we observe in peak annual loss years. Likewise, our connectivity interpretation is conceptually consistent with the scale-dependent connectivity framework of Urban and Keitt (2001) and with the notion of critical scales in fragmented landscapes highlighted by Keitt et al. (1997). Together, these links support the external validity of the triadic reading (complexity - fragmentation/disorder - heterogeneity/connectivity).

### ***Geographical and ecological implications***

The Romanian forest matrix in the Banat Mountains remains highly compact, yet the accumulation of loss is reorganising the mosaic toward more intricate, edge-rich patch boundaries and less lacunar gaps; such edge proliferation under fragmentation is well documented in landscape-metric frameworks and edge-effect syntheses (McGarigal et al., 2012c). Ecologically, these changes can reconfigure habitat connectivity, with graph-theoretic analyses showing that small structural shifts can alter functional linkages among patches (Urban & Keitt, 2001). They may also affect hydrological regulation by changing

evapotranspiration, infiltration, and moisture recycling, with wide-ranging consequences for flows and microclimate (Bruijnzeel, 2004). Disturbance resilience tends to decline as fragmentation intensifies, and systems become more sensitive to shock events - consistent with theory and syntheses on disturbance-driven thresholds in space and time (Turner, 2010). The identification of critical years in our series underscores this sensitivity to episodic pressures, while the volumetric sparseness of loss areas helps explain why connectivity gains remain modest and non-connecting; once certain fragmentation thresholds are crossed, recovery pathways may narrow (With & King, 1999).

Beyond the Banat Mountains, the methodological framework and the observed coupling–decoupling patterns are directly transferable to neighbouring regions such as the Serbian Carpathians and the Dinaric Alps, where similar relief energy, lithological heterogeneity, and mixed-use forest economies shape fragmentation pressures. In practice, the same letter-coded portfolio can be applied to Global Forest Change layers and national forest inventories to track (i) annual shock sensitivity, (ii) cumulative reorganisation of edges and gaps, and (iii) background matrix stability-supporting harmonised, cross-border monitoring.

### ***Methodological considerations and indicator selection***

Two methodological points merit emphasis. First, redundancy within the lacunarity pair argues for a parsimonious choice (Roy & Perfect, 2014) in routine monitoring, while retaining a succolarity reservoir variant when permeability matters. Second, global complexity can be summarised efficiently by a representative Box-counting implementation (TruSoft International, 1997; Vuidel et al., 2022; Ahammer et al., 2023) plus an Informational/Correlation dimension (Grassberger & Procaccia, 1983); FFDI is a robust proxy for branching irregularity (Peptenatu et al., 2023) and FTI for tentacular extension (Andronache et al., 2024). These choices are consistent with the observed within- and between-family correlations and with external reports (Andronache, 2024). Together, these indices complement class-level FRAGSTATS metrics (edge density, clumpiness), adding scale-aware diagnostics of edge irregularity and tentacular growth.

### ***Limitations***

Thresholding and spatial resolution influence several indices; 3D metrics additionally depend on voxelization choices (e.g., voxel size and structuring kernels). Voxelization maps the 2D raster grid into a 3D lattice; consequently, voxel dimensions (including any anisotropy between horizontal and vertical resolution) directly affect the absolute magnitude of volumetric indices. In this study, cubic voxels were employed (horizontal resolution equals vertical voxel size), allowing 3D metrics to be interpreted comparatively across layers (tree cover, cumulative loss, annual loss). Although absolute index values would rescale under different voxel dimensions, the relative contrasts and ordering of metrics remain stable. For very sparse volumes, succolarity cannot be computed and is therefore undefined. The near-constancy (low variance) of the tree-cover matrix may amplify method-specific contrasts among fragmentation metrics. Machine-learning-based gap filling (e.g., 3D denoising or interpolation) could be explored as a preprocessing step, but it was not applied here because it may alter fine-scale structure and connectivity. Any ML-based reconstruction would require dedicated validation of induced artifacts and uncertainty; therefore, we note it only as an optional future enhancement. These caveats notwithstanding, the strong convergence between 2D and 3D signals, and the stable correlation architecture across layers, support the robustness of the triadic interpretation and of the main conclusions.

## **Synthesis**

Across scales and indicators, the organisation of the forest mosaic has changed more profoundly than its total area alone would suggest. As losses accumulate, the mosaic becomes more intricate and more disordered, gaps are less lacunar, and void connectivity rises episodically without pervasive connectivity. At annual scales, shocks transiently increase disorder and connectivity while eroding anisotropy. In the background matrix, stability attenuates correlations and exposes definition-level differences among fragmentation metrics. This integrated reading consolidates the complexity - fragmentation - connectivity triad as a unified framework for interpreting forest dynamics in the Banat Mountains and, by extension, for designing parsimonious, yet sensitive, monitoring portfolios for structurally dynamic landscapes.

## **Conclusion**

This study advances the interpretation of 2D and 3D binary images for structurally dynamic landscapes by organizing a broad set of fractal and non-fractal indices into a complementary triad - global complexity, fragmentation/disorder, and heterogeneity - connectivity (lacunarity-succolarity), applied to the Banat Mountains.

(i) Annual vs. cumulative dynamics. At annual scale, disturbance years show sharp, transient increases in fragmentation/disorder (FFDI, FTI) and momentary gains in connectivity (succolarity), accompanied by loss of directional coherence; global dimensions respond only partially. At cumulative scale, relations tighten: global complexity rises steadily, edges become more irregular and tentacular, lacunarity (heterogeneity of gaps) declines, and succolarity (patch-to-patch connectivity) increases modestly without reaching landscape-scale connectivity.

(ii) Stable matrix and method sensitivity. Tree cover behaves as a compact, nearly space-filling matrix in 2D and 3D, with low and stable fragmentation and high, stable connectivity; under low variance, definition-level differences among fragmentation metrics (FFI vs. FFDI/FTI) become visible.

(iii) Convergence across dimensions. The 3D analysis corroborates the 2D reading: tree cover is volumetrically dense and coherent; cumulative loss is intermediate and filamentary; annual loss remains sparse. Succolarity is meaningful for the matrix but undefined for very sparse loss volumes.

A compact monitoring portfolio includes one representative box-counting implementation + an Informational/Correlation dimension (global complexity); FFDI + FTI (fragmentation/disorder and tentacularity); Roy & Perfect lacunarity with a succolarity (reservoir) variant when connectivity is of specific interest; include directional descriptors where shocks are expected.

Results may depend on thresholding, resolution, and voxelization; succolarity becomes undefined in sparse volumes; anisotropy could be further resolved with full-azimuth (0-360°) analyses. Priorities include uncertainty quantification, sensitivity analyses, generalized/multifractal spectra, and cross-site validation linking structure to ecological function. More broadly, the multi-metric triad offers a practical basis for assessing forest-landscape sustainability across Southeastern Europe, enabling consistent benchmarking, uncertainty-aware reporting, and policy-relevant comparisons across jurisdictions.

Data and code availability: All binary layers, parameter files, and analysis scripts are provided in the supplementary material. Summary CSV outputs and the letter legend (a-af) are included to ensure full reproducibility.

Acknowledgments: The authors are grateful to the anonymous reviewers for their valuable contributions.

Conflict of Interest: The authors declare no conflict of interest.

Publisher's Note: Serbian Geographical Society stays neutral with regard to jurisdictional claims in published maps and institutional affiliations.

© 2026 Serbian Geographical Society, Belgrade, Serbia.

This article is an open access article distributed under the terms and conditions of the Creative Commons Attribution-NonCommercial-NoDerivs 3.0 Serbia.

## References

- Ahammer, H., & Mayrhofer-Reinhartshuber, M. (2012). Image pyramids for calculation of the box-counting dimension. *Fractals*, 20(03n04), 281-293. <https://doi.org/10.1142/S0218348X12500260>
- Ahammer, H., Reiss, M. A., Hackhofer, M., Andronache, I., Radulovic, M., Labra-Spröhnle, F., & Jelinek, H. F. (2023). ComsystemJ: A collection of Fiji/ImageJ2 plugins for non-linear and complexity analysis in 1D, 2D and 3D. *PLOS ONE*, 18(10), Article e0292217. <https://doi.org/10.1371/journal.pone.0292217>
- Andronache, I. (2024). Analysis of Forest Fragmentation and Connectivity Using Fractal Dimension and Succolarity. *Land*, 13(2), Article 138. <https://doi.org/10.3390/land13020138>
- Andronache, I. C., Ahammer, H., Jelinek, H. F., Peptenatu, D., Ciobotaru, A.-M., Draghici, C. C., Pintilii, R. D., Simion, A. G., & Teodorescu, C. (2016). Fractal analysis for studying the evolution of forests. *Chaos, Solitons & Fractals*, 91, 310-318. <https://doi.org/10.1016/j.chaos.2016.06.013>
- Andronache, I., Marin, M., Fischer, R., Ahammer, H., Radulovic, M., Ciobotaru, A.-M., Jelinek, H. F., Di Ieva, A., Pintilii, R.-D., Drăghici, C.-C., Herman, G. V., Nicula, A.-S., Simion, A.-G., Loghin, I.-V., Diaconu, D.-C., & Peptenatu, D. (2019). Dynamics of Forest Fragmentation and Connectivity Using Particle and Fractal Analysis. *Scientific Reports*, 9(1), Article 12228. <https://doi.org/10.1038/s41598-019-48277-z>
- Andronache, I., Peptenatu, D., Ahammer, H., Radulovic, M., Djuričić, G. J., Jelinek, H. F., Russo, C., & Di Ieva, A. (2024). Fractals in the Neurosciences: A Translational Geographical Approach. In A. Di Ieva (Eds.), *The Fractal Geometry of the Brain* (Vols. 1-2, pp. 953-981). Springer International Publishing. [https://doi.org/10.1007/978-3-031-47606-8\\_47](https://doi.org/10.1007/978-3-031-47606-8_47)
- Artugyan, L. (2016). Geomorphosites Assessment in Karst Terrains: Anina Karst Region (Banat Mountains, Romania). *Geoheritage*, 9(2), 153-162. <https://doi.org/10.1007/s12371-016-0188-x>
- Bruijnzeel, L. A. (2004). Hydrological functions of tropical forests: Not seeing the soil for the trees? *Agriculture, Ecosystems & Environment*, 104(1), 185-228. <https://doi.org/10.1016/j.agee.2004.01.015>

- Cojocariu, L. L., Copăcean, L., Ursu, A., Sărățeanu, V., Popescu, C. A., Horablaga, M. N., Bordean, D.-M., Horablaga, A., & Bostan, C. (2024). Assessment of the Impact of Population Reduction on Grasslands with a New “Tool”: A Case Study on the “Mountainous Banat” Area of Romania. *Land*, 13(2), Article 134. <https://doi.org/10.3390/land13020134>
- de Melo, R. H. C., & Conci, A. (2013). How Succolarity could be used as another fractal measure in image analysis. *Telecommunication Systems*, 52(3), 1643-1655. <https://doi.org/10.1007/s11235-011-9657-3>
- Diaconu, D. C., Andronache, I., Gruia, A. R., Bazac, T., & Băloi, A. M. (2024). Evaluation of forest loss data using fractal algorithms: Case study Eastern Carpathians-Romania. *Frontiers in Forests and Global Change*, 7, Article 1432739. <https://doi.org/10.3389/ffgc.2024.1432739>
- Dubuc, B., Zucker, S. W., Tricot, C., Quiniou, J. F., & Wehbi, D. (1989). Evaluating the fractal dimension of surfaces. *Proceedings of the Royal Society of London. A. Mathematical and Physical Sciences*, 425(1868), 113-127. <https://doi.org/10.1098/rspa.1989.0101>
- Grassberger, P., & Procaccia, I. (1983). Measuring the strangeness of strange attractors. *Physica D: Nonlinear Phenomena*, 9(1-2), 189-208. [https://doi.org/10.1016/0167-2789\(83\)90298-1](https://doi.org/10.1016/0167-2789(83)90298-1)
- Gustafson, E. J. (2019). How has the state-of-the-art for quantification of landscape pattern advanced in the twenty-first century? *Landscape Ecology*, 34(9), 2065-2072. <https://doi.org/10.1007/s10980-018-0709-x>
- Halley, J. M., Hartley, S., Kallimanis, A. S., Kunin, W. E., Lennon, J. J., & Sgardelis, S. P. (2004). Uses and abuses of fractal methodology in ecology. *Ecology Letters*, 7(3), 254-271. <https://doi.org/10.1111/j.1461-0248.2004.00568.x>
- Hansen, M. C., Potapov, P. V., Moore, R., Hancher, M., Turubanova, S. A., Tyukavina, A., Thau, D., Stehman, S. V., Goetz, S. J., Loveland, T. R., Kommareddy, A., Egorov, A., Chini, L., Justice, C. O., & Townshend, J. R. G. (2013). High-Resolution Global Maps of 21st-Century Forest Cover Change. *Science*, 342(6160), 850-853. <https://doi.org/10.1126/science.1244693>
- Haralick, R. M., Shanmugam, K., & Dinstein, I. (1973). Textural Features for Image Classification. *IEEE Transactions on Systems, Man, and Cybernetics*, SMC-3(6), 610-621. <https://doi.org/10.1109/TSMC.1973.4309314>
- Ianăș, A.-N. (2013). Landscape Quality Assessment in Almăj Land Rural System from the Mountainous Banat (Romania), during the 1990-2010 period. *Forum Geografic*, 12(1), 43-51. <https://doi.org/10.5775/fg.2067-4635.2013.034.i>
- Ianăș, A.-N., & Ivan, R. (2022). Post-communist land cover and use changes in Romanian Banat, based on CORINE Land Cover data. *Review of Historical Geography and Toponomastics*, XVII(33-34), 155-174.
- Janda, P., Trotsiuk, V., Mikoláš, M., Bače, R., Nagel, T. A., Seidl, R., Seedre, M., Morrissey, R. C., Kuchel, S., Jaloviar, P., Jasík, M., Vysoký, J., Šamonil, P., Čada, V., Mrhalová, H., Lábusová, J., Nováková, M. H., Rydval, M., Matějů, L., & Svoboda, M. (2017). The historical disturbance regime of mountain Norway spruce forests in the Western Carpathians and its influence on current forest structure and composition. *Forest Ecology and Management*, 388, 67-78. <https://doi.org/10.1016/j.foreco.2016.08.014>
- Jin, X. C., Ong, S. H., & Jayasooriah. (1995). A practical method for estimating fractal dimension. *Pattern Recognition Letters*, 16(5), 457-464. [https://doi.org/10.1016/0167-8655\(94\)00119-N](https://doi.org/10.1016/0167-8655(94)00119-N)

- Karperien, A. (2015). *FracLac for ImageJ* (<http://rsb.info.nih.gov/ij/plugins/frac-lac/FLHelp/Introduction.htm>; Version 2015Sep090313a9330) [Java]. Charles Sturt University; <http://rsb.info.nih.gov/ij/plugins/frac-lac/FLHelp/Introduction.htm>
- Keitt, T. H., Urban, D. L., & Milne, B. T. (1997). Detecting critical scales in fragmented landscapes. *Conservation Ecology*, 1(1), 4-4.
- Knorn, J., Kuemmerle, T., Radeloff, V. C., Keeton, W. S., Gancz, V., Biriş, I.-A., Svoboda, M., Griffiths, P., Hagatis, A., & Hostert, P. (2013). Continued loss of temperate old-growth forests in the Romanian Carpathians despite an increasing protected area network. *Environmental Conservation*, 40(2), 182-193. <https://doi.org/10.1017/S0376892912000355>
- Landini, G., & Rippin, J. W. (1993). Notes on the implementation of the mass - radius method of fractal dimension estimation. *Bioinformatics*, 9(5), 547-550. <https://doi.org/10.1093/bioinformatics/9.5.547>
- Mandelbrot, B. B. (1982). *The fractal geometry of nature*. W.H. Freeman.
- Mayrhofer-Reinhartshuber, M., Kainz, P., & Ahammer, H. (2013). Image Pyramids as a new approach for the determination of fractal dimensions. *Proceedings of the 2nd International Conference on Pattern Recognition Applications and Methods*, 239-243. <https://doi.org/10.5220/0004325902390243>
- McGarigal, K., Cushman, S. A., & Ene, E. (2012). *FRAGSTATS v4: Spatial Pattern Analysis Program for Categorical and Continuous Maps*. University of Massachusetts Amherst, Massachusetts, USA. <https://www.fragstats.org/>
- Milne, B. T. (1988). Measuring the fractal geometry of landscapes. *Applied Mathematics and Computation*, 27(1), 67-79. [https://doi.org/10.1016/0096-3003\(88\)90099-9](https://doi.org/10.1016/0096-3003(88)90099-9)
- Milne, B. T. (1991). Lessons from applying fractal models to landscape patterns. In M. G. Turner & R. H. Gardner (Eds.), *Quantitative Methods in Landscape Ecology* (pp. 199-235). Springer-Verlag.
- Newman, E. A., Kennedy, M. C., Falk, D. A., & McKenzie, D. (2019). Scaling and Complexity in Landscape Ecology. *Frontiers in Ecology and Evolution*, 7, 293. <https://doi.org/10.3389/fevo.2019.00293>
- O'Neill, R. V., Krummel, J. R., Gardner, R. H., Sugihara, G., Jackson, B., DeAngelis, D. L., Milne, B. T., Turner, M. G., Zygmunt, B., Christensen, S. W., Dale, V. H., & Graham, R. L. (1988). Indices of landscape pattern. *Landscape Ecology*, 1(3), 153-162. <https://doi.org/10.1007/BF00162741>
- Peptenatu, D., Andronache, I., Ahammer, H., Radulovic, M., Costanza, J. K., Jelinek, H. F., Di Ieva, A., Koyama, K., Grecu, A., Gruia, A. K., Simion, A.-G., Nedelcu, I. D., Olteanu, C., Drăghici, C.-C., Marin, M., Diaconu, D. C., Fensholt, R., & Newman, E. A. (2023). A new fractal index to classify forest fragmentation and disorder. *Landscape Ecology*, 38(6), 1373-1393. <https://doi.org/10.1007/s10980-023-01640-y>
- Petrişor, A.-I., Ianoş, I., & Tălângă, C. (2010). Land cover and use changes focused on the urbanization processes in Romania. *Environmental Engineering and Management Journal*, 9(6), 765-771.
- Plotnick, R. E., Gardner, R. H., & O'Neill, R. V. (1993). Lacunarity indices as measures of landscape texture. *Landscape Ecology*, 8(3), 201-211. <https://doi.org/10.1007/BF00125351>
- Posea, G. (2005). *Geomorfologia României: Relief - tipuri, geneză, evoluție, regiunare* (Ediția a 2-a revăzută și adăugită). Editura Fundației „România de Măine”.

- QGIS Development Team. (2024). *QGIS Geographic Information System* [Computer software]. Open Source Geospatial Foundation Project. <http://qgis.osgeo.org>
- Reiss, M. A., Lemmerer, B., Hanslmeier, A., & Ahammer, H. (2016). Tug-of-war lacunarity - A novel approach for estimating lacunarity. *Chaos: An Interdisciplinary Journal of Nonlinear Science*, 26(11), Article 113102. <https://doi.org/10.1063/1.4966539>
- Roy, A., & Perfect, E. (2014). Lacunarity analyses of multifractal and natural grayscale patterns. *Fractals*, 22(03), Article 1440003. <https://doi.org/10.1142/S0218348X14400039>
- Sarkar, N., & Chaudhuri, B. B. (1992). An efficient approach to estimate fractal dimension of textural images. *Pattern Recognition*, 25(9), 1035-1041. [https://doi.org/10.1016/0031-3203\(92\)90066-R](https://doi.org/10.1016/0031-3203(92)90066-R)
- Sasaki, H., Shibata, & Hatanaka, T. (1994). Method for evaluation of Japanese lawn grass (*Zoysia japonica* Steud.) ecotypes for different purposes. *Bulletin of the National Grassland Research Institute (Japan)*, 49, 17-24.
- Schertzer, D., & Lovejoy, S. (2011). Multifractals, generalized scale invariance and complexity in geophysics. *International Journal of Bifurcation and Chaos*, 21(12), 3417-3456. <https://doi.org/10.1142/S0218127411030647>
- Schneider, C. A., Rasband, W. S., & Eliceiri, K. W. (2012). NIH Image to ImageJ: 25 years of image analysis. *Nature Methods*, 9(7), 671-675. <https://doi.org/10.1038/nmeth.2089>
- TruSoft International. (1997). *Benoit* (Version 1.31) [Computer software]. TruSoft Int'l Inc; <https://www.trusoft-international.com>. <http://www.trusoft-international.com/benoit.html>
- Turcotte, D. L. (1997). *Fractals and Chaos in Geology and Geophysics* (2nd ed.). Cambridge University Press. <https://doi.org/10.1017/CBO9781139174695>
- Turner, M. G. (2010). Disturbance and landscape dynamics in a changing world. *Ecology*, 91(10), 2833-2849. <https://doi.org/10.1890/10-0097.1>
- Urban, D., & Keitt, T. (2001). Landscape connectivity: A graph-theoretic perspective. *Ecology*, 82(5), 1205-1218. [https://doi.org/10.1890/0012-9658\(2001\)082%255B1205:LCAGTP%255D2.o.CO;2](https://doi.org/10.1890/0012-9658(2001)082%255B1205:LCAGTP%255D2.o.CO;2)
- Vuidel, G., Frankhauser, P., & Tannier, C. (2022). *Fractalyse: A Fractal Analysis Software* (Version 3.0) [Java]. ThéMA laboratory.
- With, K. A., & King, A. W. (1999). Extinction Thresholds for Species in Fractal Landscapes. *Conservation Biology*, 13(2), 314-326. <https://doi.org/10.1046/j.1523-1739.1999.013002314.x>
- Zmeškal, O., Veselý, M., Martin Nežádal, & Buchniček, M. (2011). Fractal Analysis of Images Structures. *HarFA E-Journal*, 3-5.